

A Planar Approach for Manufacturing Cardiac Stents: Design, Fabrication, and Mechanical Evaluation

Kenichi Takahata and Yogesh B. Gianchandani, *Member, IEEE*

Abstract—A new approach that uses planar batch manufacturing technologies is presented for the design and fabrication of coronary artery stents. Stent samples with different wall patterns have been fabricated from 50- μm -thick stainless steel foil using microelectrodischarge machining. Stents have been expanded to tubular shapes by using angioplasty balloons, both inside mock arteries and without external confinement (i.e., free-standing). Free-standing stents exhibit diameter variations of $<\pm 4\%$, almost zero radial recoil after deflation of the balloon, and longitudinal shrinkage of $<3\%$ upon expansion. A variation that uses breakable links to provide additional customization in electrical and mechanical properties is also presented. Loading tests reveal that the radial stiffness of some patterns is comparable to that of commercially available stents with greater wall thickness, while bending compliance, at 0.02 m/N for a 4-mm-long section of the stent, is also favorably large. [1080]

Index Terms—Angioplasty, arc, electrodischarge, micro-machining, stent.

I. INTRODUCTION

STENTS are mechanical devices that are chronically implanted into arteries in order to physically expand and scaffold blood vessels that have been narrowed by plaque accumulation. Although they have found the greatest use in fighting coronary artery disease, stents are also used in blood vessels and ducts in other parts of the body. These include iliac arteries [1], carotid arteries [2], renal arteries [3], biliary ducts [4] and ureters [5]. Although different stent applications have varying requirements of design, form factor, and mechanical performance which may put certain constraints on the manufacturing and assembly approaches that can be used for them, the vast majority of coronary stents are made by laser machining and subsequent electropolishing of stainless steel tubes [6], creating mesh-like walls that allow the tube to be expanded radially with a balloon that is inflated during the medical procedure, known as balloon angioplasty. This fabrication approach is serial in nature and prevents the use of substantial resources available for fabricating planar microstructures.

Microelectrodischarge machining (μEDM) provides an alternate approach for cutting metal microstructures. This technique is capable of performing 3-D micromachining in any electrical conductor with sub-micron tolerance and surface smoothness. It

involves the sequential discharge of controlled electrical pulses between a microscopic electrode and a sample in dielectric fluid. These pulses cut into the sample, but also contribute to the erosion of the electrode. Conventionally, the μEDM electrode is formed by the shaped end of a narrow-gauge wire. When machining at a single spot, it is advanced into the sample at rate of 1–5 $\mu\text{m/s}$. When machining a surface, it scrolled across the sample at a rate about 1.5 mm/s and advanced into the sample at a reduced rate of 0.1–0.5 $\mu\text{m/s}$.

The μEDM method has not been extensively used for stent production in the past because traditional μEDM that uses single electrodes with single pulse timing circuits often suffers from even lower throughput than the laser machining. However, it has been recently demonstrated that both the throughput and the tolerance of μEDM can be significantly improved by using spatial and temporal parallelism, i.e., using lithographically formed arrays of planar electrodes with free-running and independent discharge sequences generated with the help of on-chip parasitic capacitances [7]. Thus, any structure cut by μEDM from a planar foil is compatible with lithographic manufacturing. This paper reports a new fabrication approach that uses metal foils as starting materials for stents, which permits this parallelism to be exploited, thereby offering high throughput, precision, and repeatability¹. The favored mechanical characteristics of radial stiffness and longitudinal or bending compliance in expanded stents have been experimentally and theoretically investigated, and are discussed with comparisons to commercial stents. A variation that uses strategically located breakable links in the stent provides additional freedom in customizing the mechanical and electrical properties of these devices.

II. DESIGN AND FABRICATION

The fabrication approach was to μEDM 50- μm -thick stainless steel foil into a structure that could be slipped over an angioplasty balloon and reshaped into a cylinder when deployed in the manner of a conventional stent. The design challenge was to develop a planar pattern which would provide the critical mechanical characteristics of radial stiffness and bending compliance in the expanded structure. In order to reduce the likelihood of joint failure, it was decided to develop a structure that was completely flexural in nature, and did not have any bonded or hinged joints. This effort used 50- μm -thick type 304 stainless steel, which is readily available in the flatness and size required for μEDM and has mechanical properties that are almost identical to the type 316 stainless steel commonly used in commercially available stents.

Manuscript received June 26, 2003; revised April 6, 2004. This work is supported in part by a grant from the National Science Foundation. Subject Editor D. J. Beebe.

The authors are with the Department of Electrical Engineering and Computer Science, The University of Michigan, Ann Arbor, MI 48108-2122 USA (e-mail: ktakahat@eecs.umich.edu).

Digital Object Identifier 10.1109/JMEMS.2004.838357

¹Portions of this paper have appeared in conference abstract form in [8].

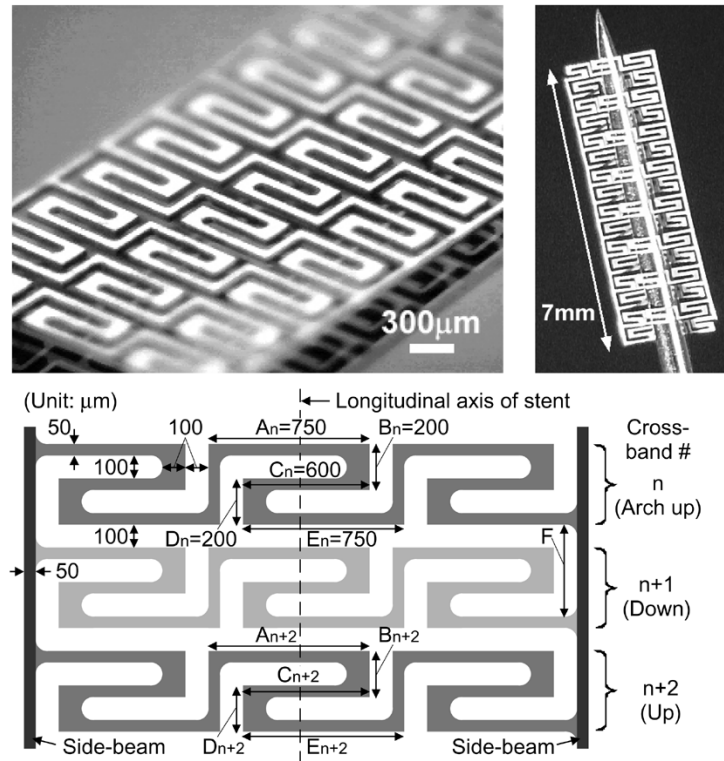


Fig. 1. Pre-expansion form of a UMich stent design 1. (a) Upper left: a fabricated sample as cut from the metal foil. (b) Upper right: a needle weaved through the metal foil showing the alternating cross-bands. (c) Lower: a wall pattern layout with involute-shaped cross-bands and its dimensions.

Several layouts were designed and experimentally tested. The best results in terms of mechanical characteristics (discussed in Section III) were obtained with the design shown in Fig. 1, which will be referred to as design 1. The pattern has two longitudinal side-beams, which are connected transversely by cross-bands [Fig. 1(c)], each of which contains three identical involute loops. The involute shape is tailored to provide selected stress-relief during expansion of the stent to the deployment diameter, which is 2.65 mm in this case. In order to increase radial stiffness, this design uses a larger number of cross-bands per unit length of the stent and beams A_n , C_n , and E_n are designed to be longer than the others, B_n and D_n .

Another representative layout is illustrated in Fig. 2, which will be referred to as design 2. It has similar dimensions and a configuration that uses an array of cross-bands and two side-beams, but the cross-bands have a switchback pattern in this case. In contrast to the involute design, the beam segments G , which are parallel to the longitudinal axis, are longer than segments H , which are perpendicular to the axis. This design, in general, has a higher expansion ratio to the initial width between side-beams in radial direction, but fewer cross-bands along the longitudinal axis.

In this initial effort, μ EDM patterning of the stainless steel foil was performed with the conventional scanning method using cylindrical electrodes of 50–100 μ m diameter shaped from metal wire. The use of a planar metal foil as the starting material ensured compatibility with lithography-compatible batch manufacturing. To emulate the deployment of a stent, an angioplasty balloon was threaded through the 7-mm-long planar structure of Fig. 1 such that the transverse bands alter-

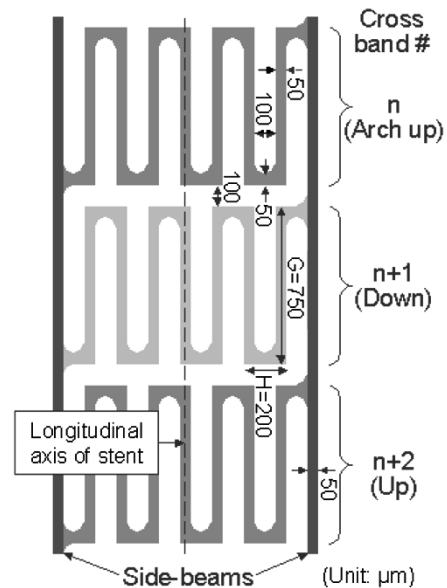


Fig. 2. Design 2 with switchback-shaped cross-bands and its dimensions.

nated above and below it, as shown in Fig. 3(a). With the set-up illustrated in Fig. 3(c), the stent was expanded by inflating the balloon with liquid up to 12 atm. pressure, in a manner identical to commercial stents, resulting in the structures shown in Fig. 3(b). Fig. 4 shows SEM images of the expanded stent with the balloon removed. Variation in the diameter of several involute-pattern samples expanded to 2.6-mm diameter was typically within $\pm 4\%$, while radial recoil upon deflation of the balloon was even smaller than that. The shrinkage in length

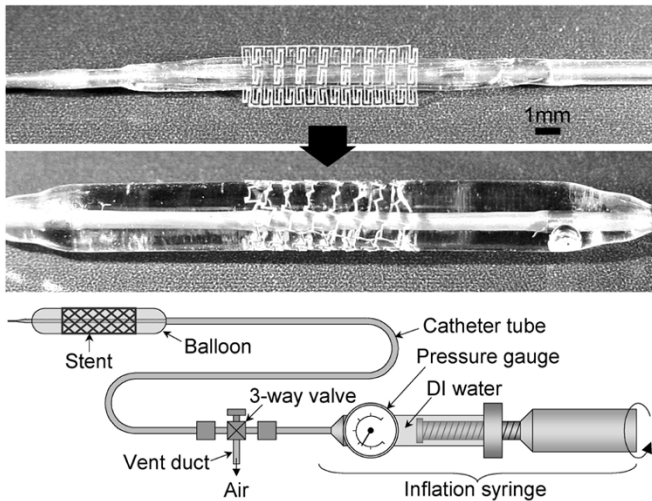


Fig. 3. Expansion of a 7-mm-long stent design 1 with an angioplasty balloon catheter. (a) Upper: the stent mounted in the deflated balloon. (b) Middle: the stent expanded with inflation of the balloon at 12 atm. (c) Lower: a set-up used for the expansion test.

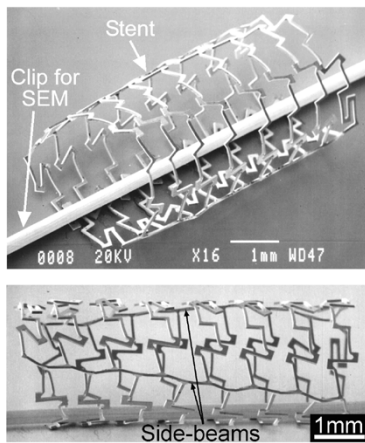


Fig. 4. SEM images of the expanded stent design 1. (a) Upper: Angled view. (b) Lower: Side view.

upon the expansion observed in the 7-mm-long stent was $<3\%$. A deployment inside a mock artery is shown in Fig. 5. The mock artery used was a commercially available silicone-based tube (Dynatek Dalta Scientific Instruments, MO, USA) with 3-mm diameter and 0.25-mm wall thickness, which is tailored to have radial compliance comparable to human coronary arteries [9]. In this deployment, the stent was expanded to 3.5-mm diameter. Fig. 5 shows that the tube has a distended sidewall at the location where the stent was deployed, demonstrating mechanical stiffness large enough to prevent the relaxation of the simulated artery.

Upon expansion of the stent, beams in the structure are permanently deformed. The pattern of the stent must, therefore, be designed to accommodate large deformations so that the maximum *tensile* stress is less than the ultimate stress, which is about 517 MPa for the 304 stainless steel [10]. The deformation and resultant stresses were evaluated by using an FEA package, ANSYS™. The simulation used a bilinear stress-strain model, and the following mechanical properties of the steel [10], [11]:

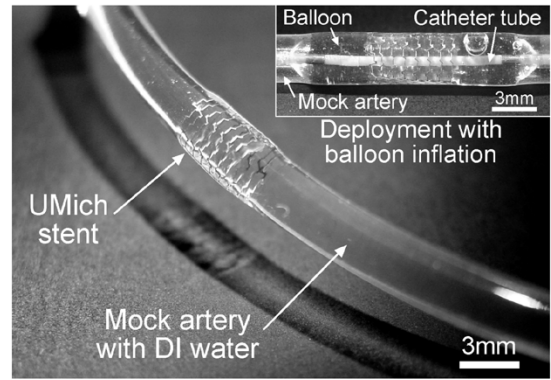


Fig. 5. Optical image of a UMich stent design 1 deployed inside a silicone mock artery, showing the distended sidewall. Inset shows the deployment with the balloon catheter.

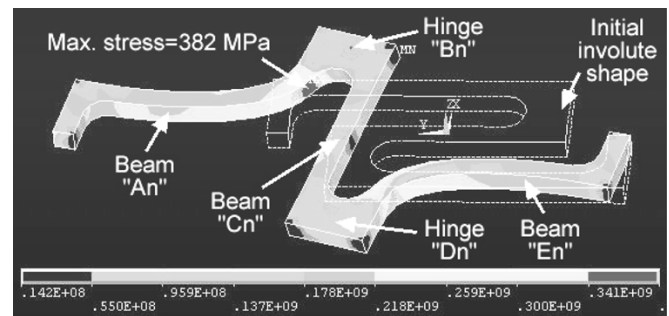


Fig. 6. FEA result for von Mises stress in a deformed involute beam due to expansion.

Young's modulus = 193 GPa, yield stress = 207 MPa, tangent modulus = 692 MPa, and Poisson's ratio = 0.27. Fig. 6 shows a unit involute section of the cross-bands of design 1 with a displacement that approximately corresponds to the deployed diameter. The maximum von Mises stress appears at the location indicated near the flexural hinge element B_n and is 382 MPa, sufficiently below the ultimate stress.

In addition to the bending of beam segments, torsional deformations also play important roles in expanding a stent and maintaining its final shape. The most significant ones are in the side-beams, which are twisted by $90\text{--}180^\circ$ along the segment F [labeled in Fig. 1(c)] between two adjacent bands as shown in Fig. 7(a). Fig. 7(b) shows a different torsional deformation observed at a flexural hinge H in design 2. The approximate *shear* strain for both these cases is shown in Fig. 8 on a shear stress versus shear strain response curve for 304L stainless steel obtained from [12]. It is evident that beam fracture associated with only the torsion is not a concern for the stent. For the test in Fig. 7(b), the hinges as well as the beams had $50\text{-}\mu\text{m}$ -square cross section. Although the strain due to this torsion is well below the fracture point, additional deformations at the site also include bending that may further increase the maximum strain experienced. Fig. 9 shows a mechanical failure due to combination of severe bending and tension. This fracture was observed in design 1_A , a precursor to design 1 for which width of flexural hinges was $50\ \mu\text{m}$, and segments A_n (and E_n), B_n (and D_n), and C_n were 550, 150, and $450\ \mu\text{m}$ respectively. The narrower width and shorter length in the flexural hinges B_n and D_n , of

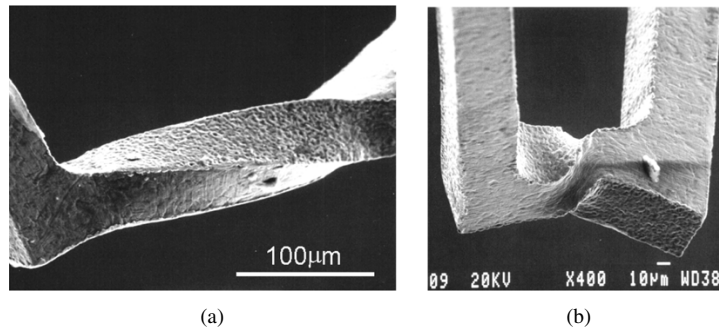


Fig. 7. Plastic deformation in torsion (a) at segment F of a side beam in design 1 and (b) at a flexural hinge H in design 2.

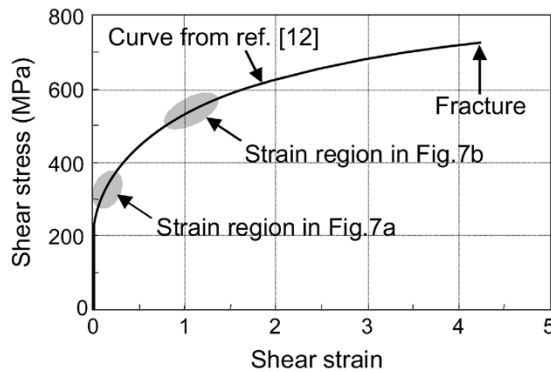


Fig. 8. Shear stress-strain curve for 304L stainless steel and approximate strain regions seen in Fig. 7.

this design contribute to an increase in the tensile stress at the hinge. Since this was the only failure experienced during the entire research effort, it is likely that an instance of metallurgical defect may have contributed to it. Note that in design 1 a larger safety margin to the fracture point was incorporated by two changes: i) doubling the widths of the segments B_n and D_n from 50 to 100 μm and ii) increasing the lengths of the same segments from 150 to 200 μm by doubling the gap between adjacent beams as seen in Fig. 1(c). These increments in length and width of the structural beams in design 1 may compromise radial stiffness compared to design 1_A when both are expanded to the same diameter. Thus, there is an indirect compromise between the radial stiffness and the safety margin.

In addition to stents, this planar approach can be used for the fabrication of 3-D inductors. The final structure of stents is essentially a set of series-connected rings which offers negligible inductance. Use of breakable links [Fig. 10(a)] permits formation of helical coils in the same manner for the deployment of stents. When the balloon is inflated for expanding the planar structure, torsional strain developed in the side-beams is effectively concentrated at the links made in the beams [Fig. 10(b)], leading to fracture [Fig. 10(c)]. The resultant final shape can be helical by placing the links at selected locations. Note that this fracture is *controlled* breakage as opposed to that in Fig. 9, and the fractured cross section area is minimal as displayed in comparison between Figs. 9 and 10(c). This technique opens a path for a stent to serve as an electrical component, such as an antenna, for wireless communication with an implantable microsystem that measures blood pressure and flow rate.

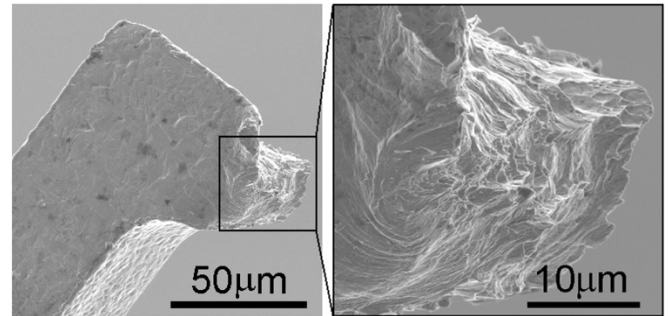


Fig. 9. Unintended fracture at a flexural hinge in design 1_A. The close-up shows the fractured cross section.

III. EXPERIMENTAL RESULTS

Radial stiffness is a paramount mechanical characteristic in the stents. Several past efforts have assessed the stiffness of commercial stents [13], [14]. To evaluate our devices, short samples for involute and switchback designs were prepared and subjected to loading tests in which the reaction force of the stent (per unit length) was measured as a function of radial deformation. A sample was held in a groove mounted on the stage and compressed toward the probe (Fig. 11). The gauge was rigidly fixed, and the displacement of the gauge probe was negligible compared to that of the sample. The force was measured by a gauge (Imada Inc., IL, USA, DPS-1) that provides 1-mN resolution while first compressing the stent by 1.5 mm in 25 μm increments, and then while relaxing the deformation.

Fig. 12 shows results of the radial stiffness test. The vertical axis represents the mechanical load that was applied to the sample. In order to permit the comparison of stents of unequal length, this is specified per unit length. The horizontal axis represents the deformation in the stent along the axis of the applied load. Measurements demonstrate that the UMich design 1_A that uses the involute cross-bands requires a force of about 0.28 N per mm of stent length in order to deform the radius by 1.5 mm. The other involute pattern (design 1) has somewhat less stiffness, which is due to the longer length of the strained segments. The switchback pattern (design 2), which has fewer cross-bands per unit length, provides less radial stiffness than the involute pattern. An 8-mm-long commercial stent (Multilink Tetra is a trademark of Guidant Co., IN, USA) with type 316L stainless steel of thickness varying over 90–130 μm was expanded to the same diameter as UMich design 1_A and tested for comparison.

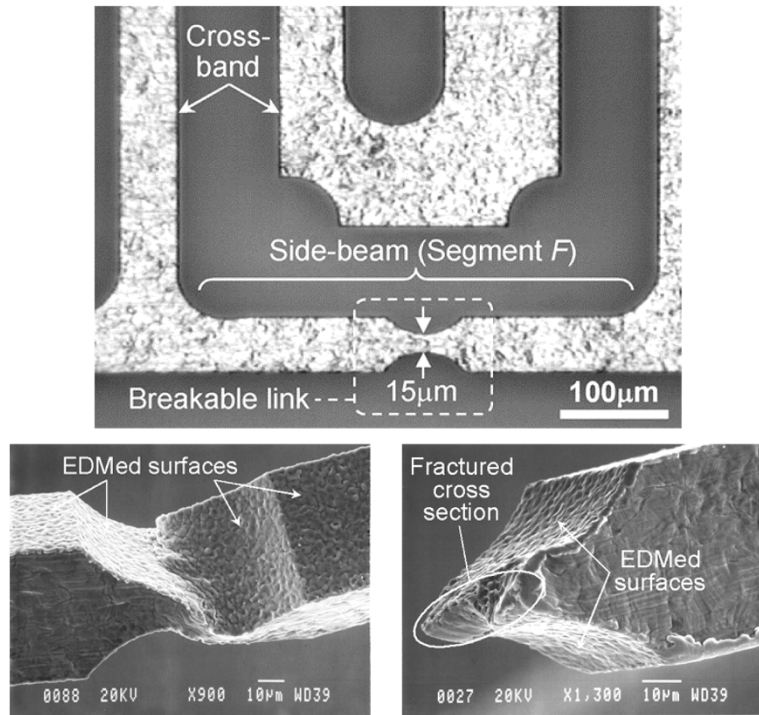


Fig. 10. (a) Upper: Optical image showing a breakable link made in a side-beam in a planar structure, as machined. (b) Lower left: Unbroken link in a device mounted on a deflated balloon. (c) Lower right: Broken link from an expanded device.

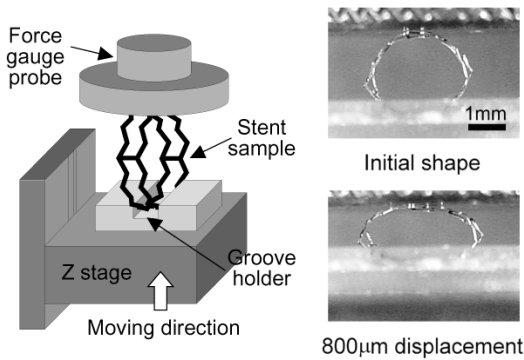


Fig. 11. (a) Left: Loading test setup and (b) Right: Sample deformation in the test.

The results, also shown in Fig. 12, were very similar for both designs, suggesting that stents fabricated by the planar approach can indeed provide comparable radial stiffness to commercial stents that serve existing needs. Additionally, it can be observed from Fig. 12 that UMich designs exhibit relatively good elastic recovery after loading, as evidenced by the lower intercept on the horizontal axis for the curves representing decreasing load.

Orientation dependence of the radial stiffness was a concern for the UMich stents since they were shaped from planar sheets. Identical samples of design 2 with four cross-bands were tested in two different orientations as shown in Fig. 13: (A) perpendicular to a plane that includes both side-beams, and (B) parallel to the plane. The measurements shown in Fig. 13 demonstrate that the radial stiffness is similar in both cases.

The experimental results in Fig. 12 show a few discontinuities in the response curve of design 1_A when deformed by 500 µm

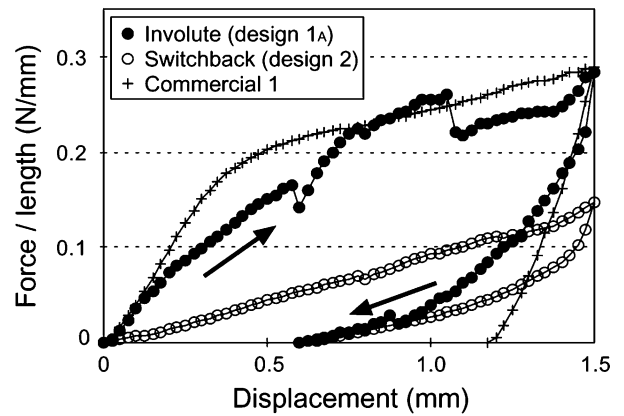


Fig. 12. Measurement of the radial stiffness of an involute pattern UMich stent and comparison to a commercial stent with similar diameter and twice the thickness.

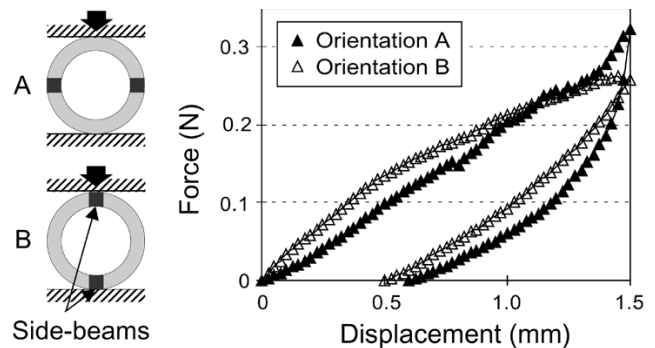


Fig. 13. Measured radial stiffness of design 2 in two different orientations for a stent of 2.6-mm diameter and 2.2-mm length.

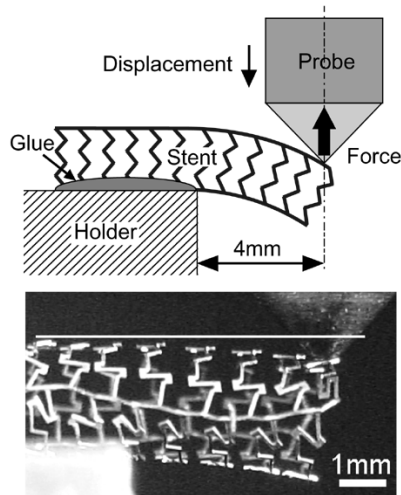


Fig. 14. (a) Upper: Setup for bending compliance test. (b) Lower: Optical micrograph of a UMich stent sample under test.

and more. While this is a substantial deformation, it is interesting to note the source of this behavior. As can be seen in Fig. 6, beams that correspond to C_n in Fig. 1(c) are designed to rotate about their center by $\sim 90^\circ$ during the expansion. As a result, hinges D_n and B_{n+2} are positioned closely to each other. In addition, alternate cross-bands in Fig. 1(c), which adjoin each other when they are mounted on the balloon, deform in a way that the gaps between their segments are reduced as the stent expands, since the side beams are deformed to wave-like shapes as seen in Fig. 4(b). The combination of these effects results in increased probability of physical contact between the hinges D_n and B_{n+2} as the balloon is being inflated. As loading is applied, hinges happen to come into contact and get intermeshed, and then snap apart as the loading is further increased. This particular sample, being design 1_A, had a reduced gap of $50 \mu\text{m}$ between the cross-bands, which could also contribute to increase the probability. This undesirable mechanical interaction, however, can be improved by optimizing the layout. It is evident from Fig. 12 that design 2 does not display discontinuities in its characteristic response for the range tested. Similarly, design 1, which was deformed by $300 \mu\text{m}$ in its tests, did not show any discontinuities over that range. It is expected that the propensity for adjacent beams to come into contact under severe loading conditions will be further mitigated when the device is placed in an artery.

Bending compliance is a favored characteristic in stents. This is because the stent, fitted on an angioplasty balloon in a state that is only slightly expanded, must often travel a convoluted path along a blood vessel in order to reach the location of the deployment. In addition, bending flexibility in a fully expanded stent can be beneficial for its deployment at curved sites. The bending compliance of the fabricated stents was tested using the set-up shown in Fig. 14(a). A fully expanded 7-mm-long stent of design 1 was attached to a holder such that a 4-mm segment out of it was overhanging and unsupported. The deflected stent is pictured in Fig. 14(b). A similar test was also applied to the commercial stent tested before. Radial deformation due to bending force was negligibly small compared to bending displacement

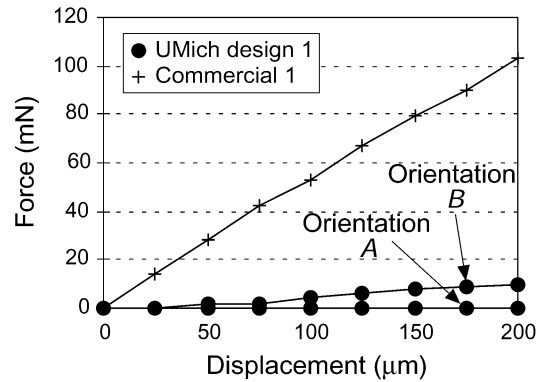


Fig. 15. Comparison of the bending compliance between UMich stent design 1 and a commercial stent.

for both the UMich and the commercial samples. The results in Fig. 15 reveal that the UMich stent had spring constants of 50 N/m and $<5 \text{ N/m}$ depending on the orientation, whereas that in the commercial stent resulted in 515 N/m . While this test was only performed on expanded stents, it suggests that the UMich stents will perform adequately in this respect.

IV. CONCLUSION

The design and fabrication of coronary artery stents based on use of planar stainless steel foil and μEDM technology has been investigated. The devices are intended to be compatible with standard stenting tools and procedures. The wall patterns were designed using FEA so that both the stress relief and the mechanical stiffness are simultaneously achieved in the expansion. Devices consist of involute bands tied between a pair of side-beams. Measurements indicate that this approach to manufacturing stents clearly has the potential to provide both the necessary radial stiffness and bending flexibility at levels comparable with or superior to existing options. Both the radial stiffness and the flexibility are found to have no significant dependence on orientation relative to the original planar direction of the foil. Dimensional variations in tubular diameter, longitudinal shrinkage, and radial recoiling in the expanded stents are at most a few percent. Further investigation will involve characteristics in mechanical reliability including metal fatigue due to repetitive contractions of and pulsatile flow in blood vessels, which can be a concern for cardiac stents fabricated from thin foil.

All devices tested in this effort were fabricated by batch-compatible μEDM , which can open a path to exploit photolithography-based fabrication resources for the stent production [7]. As an extension of this technology for manufacturing stents, the use of strategically located breakable links introduced in this effort will also facilitate fabrication of other 3D structures such as antennas and transformers.

ACKNOWLEDGMENT

The authors thank Prof. M. Moscucci of the Cardiovascular Center and Prof. K. Wise and A. DeHennis of the EECS Department for discussions, and also thank V. Sankaran for his work on preparation of samples and the test setup.

REFERENCES

- [1] D. A. Leung, D. J. Spinosa, K. D. Hagspiel, J. F. Angle, and A. H. Matsumoto, "Selection of stents for treating iliac arterial occlusive disease," *J. Vasc. Interv. Radiol.*, vol. 14, pp. 137–152, 2003.
- [2] P. E. Andersen, P. Justesen, B. Elle, and O. C. Roder, "Carotid artery stenting," *J. Interv. Radiol.*, vol. 13, no. 3, pp. 71–76, 1998.
- [3] C. R. Rees, "Stents for atherosclerotic renovascular disease," *J. Vasc. Interv. Radiol.*, vol. 10, no. 6, pp. 689–705, 1999.
- [4] C. Pena and P. R. Mueller, "Metallic stents in the biliary tree," *Min. Invas. Ther. Allied Technol.*, vol. 8, no. 3, pp. 191–196, 1999.
- [5] B. K. Auge and G. M. Preminger, "Ureteral stents and their use in endourology," *Curr. Opin. Urol.*, vol. 12, no. 3, pp. 217–222, 2002.
- [6] Y. P. Kathuria, "Laser microprocessing of stent for medical therapy," in *Proc. IEEE Micromech. Human Sci.*, 1998, pp. 111–114.
- [7] K. Takahata and Y. B. Gianchandani, "Batch mode micro-electro-discharge machining," *J. Microelectromech. Syst.*, vol. 11, pp. 102–110, Apr. 2002.
- [8] —, "Coronary artery stents microfabricated from planar metal foil: Design, fabrication, and mechanical testing," in *Proc. IEEE MEMS*, 2003, pp. 462–465.
- [9] J. C. Conti, E. R. Strobe, L. M. Goldenberg, and K. S. Price, "The durability of silicone versus latex mock arteries," in *Proc. ISA Biomed. Sci. Instrum. Symp.*, vol. 37, 2001, pp. 305–312.
- [10] R. C. Hibberler, *Mechanics of Materials Third Edition*. Englewood Cliffs, NJ: Prentice-Hall, 1997.
- [11] S. N. David Chua, B. J. MacDonald, and M. S. J. Hashmi, "Finite-element simulation of stent expansion," *J. Mater. Processing Technol.*, vol. 120, pp. 335–340, 2002.
- [12] *Metals Handbook*, 9th ed., vol. 8, American Society for Metals, 1985. J. R. Newby, J. R. Davis, S. V. Refsnes, "Mechanical Testing".
- [13] F. Flueckiger, H. Sternthal, G. E. Klein, M. Aschauer, D. Szolar, and G. Kleinhapfl, "Strength, elasticity, and plasticity of expandable metal stents: In vitro studies with three types of stress," *J. Vasc. Interv. Radiol.*, vol. 5, no. 5, pp. 745–750, 1994.
- [14] R. Rieu, P. Barragan, C. Masson, J. Fuseri, V. Garitey, M. Silvestri, P. Roquebert, and J. Sainsous, "Radial force of coronary stents: A comparative analysis," *Catheter. Cardiovasc. Interv.*, vol. 46, pp. 380–391, 1999.



Kenichi Takahata received the B.S. degree in physics from Sophia University, Tokyo, Japan, in 1990 and the M.S. degree in electrical engineering from the University of Michigan, Ann Arbor, in 2004. He is currently working toward the Ph.D. degree in electrical engineering at the University of Michigan.

In 1990, he joined Matsushita Research Institute Tokyo, Inc. (Panasonic) and was with Matsushita Electric Industrial Co., Japan, until 2001. At Matsushita, he was engaged in R&D of micromechanics and microfabrication technologies including microelectrodischarge machining (μ -EDM) partially for the Japanese National Project "Micromachine Technology." In 1997, he was appointed Researcher in the International Joint Research Program supported by New Energy and Industrial Technology Development Organization (NEDO) of Japan, which explored the compatibility between μ -EDM and deep X-ray lithography (LIGA) processes at the University of Wisconsin-Madison. From 1999 to 2001, he was a Visiting Scientist at University of Wisconsin-Madison for collaboration on batch mode μ -EDM technology that utilized lithographically fabricated electrodes and its application to MEMS. He currently has 221 publications, five issued patents, and 23 pending patents in the United States and Japan. His research interests are in MEMS realized by a combination of silicon and nonsilicon based manufacturing technologies.



Yogesh B. Gianchandani (S'83–M'85) received the B.S., M.S., and after some time in industry, the Ph.D. degrees in electrical engineering, with a focus on microelectronics and MEMS.

He is presently an Associate Professor in the Electrical Engineering and Computer Science (EECS) Department at the University of Michigan, Ann Arbor. Prior to this, he was with the Electrical and Computer Engineering (ECE) Department at the University of Wisconsin, Madison. He has also held industry positions with Xerox Corporation, Microchip Technology, and other companies, working in the area of integrated circuit design. His research interests include all aspects of design, fabrication, and packaging of micromachined sensors and actuators and their interface circuits. At the University of Michigan, he serves as the director of the College of Engineering Interdisciplinary Professional Degree Program in Integrated Microsystems. He has published about 130 papers in the field of MEMS, and has about 20 patents issued or pending.

Prof. Gianchandani received a National Science Foundation Career Award in 2000. He serves on the editorial boards of *Sensors and Actuators*, *IOP Journal of Micromechanics and Microengineering*, and *Journal of Semiconductor Technology and Science*. He also served on the steering and technical program committees for the IEEE/ASME International Conference on Micro Electro Mechanical Systems (MEMS) for many years, and served as a General Co-Chair for this meeting in 2002.